ACFER 182 CHONDRULES GIVE EVIDENCE FOR DIRECT CONDENSATION OF ENSTATITE-RICH LIQUIDS FROM THE SOLAR NEBULA. M. E. Varela[1], E. Zinner[2], G. Kurat[3], D. Magnelli[1], [1]Instituto de Ciencias Astronómicas de la Tierra y del Espacio (ICATE) Av. España 1512 sur, San Juan, Argentina (evarela@icate-conicet.gob.ar), [2]Laboratory for Space Sciences and the Physics Department, Washington University, St. Louis, MO 63130, USA, [3]Mineralogisch-Petrographische Abteilung, Naturhistorisches Museum, Burgring 7, 1010 Wien, Austria (deceased).

Introduction: Acfer 182 is a member of the CH carbonaceous chondrites as introduced by Bischoff et al., [1]. The CH chondrites are characterized -among other features- by 1) a depletion a moderately volatile and highly volatile elements [e.g.,2-3], 2) small size of chondrules (<90 μm), with refractory inclusions making up a small fraction [1]. The low abundance of volatile and moderately volatile elements in chondrules in the CH chondrites could be the result of their formation by gas-liquid condensation in an impact vapour cloud [4], a condensation signature of chondrule precursors [5], or a sign that chondrules were efficiently removed from the chondrule-forming region prior to condensation of these elements [6]. Although extensive studies were performed on chondrules of the CH-like chondrites [e.g., 6-11], those on Mg-rich cryptocrystalline (CC) chondrules are scarce [e.g., 6-7]. Here we report the results of major and trace element studies of some CC chondrules in Acfer 182.

Results: Acfer I, V, VII, X and XIVa, are perfectly round cryptocrystalline (CC) and radiating pyroxene (RP) chondrule from Acfer 182 (from M 6043, NHM, Vienna), with apparent diameters varying from 45 to 140 μm in (Fig. 1).

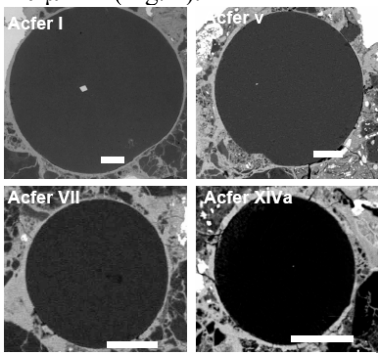

Fig. 1: Backscatter electron images of Acfer 182 CC chondrules. Bar scales represent 20 μm.

	Acfer I	Acfer V	Acfer VII	Acfer X	Acfer XIVa
N	*(10)*	*(11)*	*(10)*	*(11)*	*(14)*
SiO_2	55.5	55.7	55.3	54.1	54.3
TiO_2	0.03	0.04	0.03	0.04	0.04
Al_2O_3	0.31	0.41	0.18	0.71	0.72
Cr_2O_3	0.66	0.70	0.79	0.71	0.76
FeO	0.36	0.46	0.61	0.42	0.65
MnO	0.05	0.06	0.09	0.07	0.15
MgO	43.7	41.0	42.9	42.5	42.0
CaO	0.29	0.36	0.14	0.61	0.56
Total	100.9	98.7	100.0	99.2	99.2
Ca/Al	*1.31*	*1.16*	1.05	*1.13*	*1.05*

Major element chemistry of the chondrules is dominated by SiO_2 (54.1 – 55.7 wt%) and MgO (41 – 43.7 wt%) with minor FeO (0.65 – 0.36 wt%), Al_2O_3 (0.18 – 0.72 wt%) and CaO (0.14 -0.61 wt%) (Table).

Trace element abundances in Acfer I, V and VII are very low (0.01- ~1 x CI) and fractionated with the heavy REE (HREE) depleted (~0.01 to 0.1 x CI) relative to the light REE (LREE) (~0.2 x CI), except for Yb (in Acfer I and V), which is at the same level as the LREE (0.13 x CI). Chondrule Acfer X shows a slight REE fractionation with a positive Yb anomaly, while REE abundances of Acfer XIVa are relatively flat (~ 0.3 x CI). All objects show positive Ce and Nb anomalies and similar Sr and Ba abundances (~ 0.3 x CI) except Acfer VII (Ba ~1 x CI) (Fig 2).

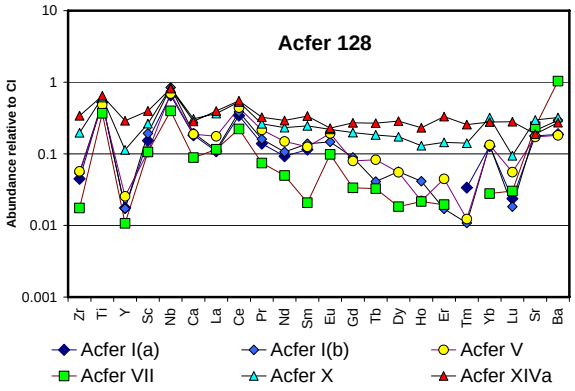

Discussion: The shapes and textures of the studied chondrules indicate that these objects once must have been liquids that were quenched, which is the basis for all major chondrule models. However, the origin of the liquids still remains unclear. The most accepted mechanisms to produce these liquids are melting of appropriate mineral precursors or direct condensation from the solar nebula.

If the studied chondrules were produced by sampling and melting of precursors, we should expect some fractionation in the CaO/Al_2O_3, Yb/La, and Sc/Yb ratios as well as some fractionation of REE (e.g., a depletion of the LREE) abundance patterns according to the mineralogy of the objects. Since the oxides Al_2O_3 and CaO are both highly refractory, they are not expected to be cosmochemically fractionated from each other. The chondritic Ca/Al ratio of the studied objects (Table) points towards a condensation origin rather than a solid precursor melting origin, in which chondrules should have sampled differing

amounts of Ca-bearing and Al-bearing precursor phases, each of which did not have a chondritic Ca/Al ratio. The direct condensation model, on the other hand, predicts a chondritic Ca/Al ratio for the early chondrules. In correlation plots between Yb and La, as well as between Yb and Sc and between Y and Zr (only Yb vs La is shown, Fig. 3) the data points of the studied CC chondrules lie close the solar ratio lines. This indicates that those elements were not fractionated during evolution of the objects due to a similar cosmochemical behavior. The fact that La has a different geochemical behavior than the two other elements (it is incompatible in contrast to Yb, which is compatible) and that in spite of this, is not fractionated from Yb, is clear evidence against geochemical fractionation.

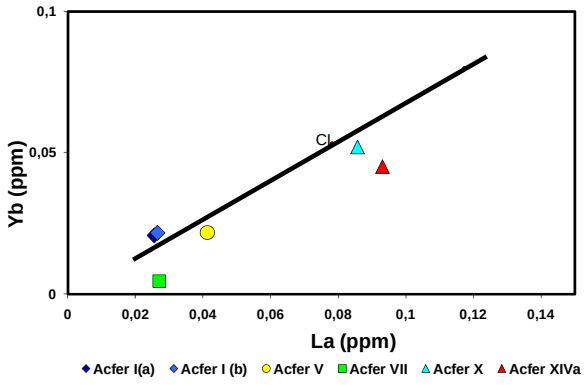

Fig. 3: The compatible/refractory element Yb is plotted against the incompatible/refractory element La.

The correlation between these elements, independent of their geochemical behavior, indicates that cosmochemical processes predominanctly determine the elemental abundances. Acfer 182 CC chondrules seem to result from direct condensation from gas into liquid.

Could some of these objects be the result of condensation from an evaporated gas of a material of chondritic composition, as indicate by the simultaneous Ce and Eu anomalies?

As shown by [12], a single-stage evaporation of an initially chondritic material produces both, Ce and Eu depletion in highly fractionated residues, similarly to those observed in the evaporation residue of synthetic perovskite [13]. However, the lack of a Yb anomaly in all fractionated residues [12] makes this formation mechanism improvable. The observed HREE/LREE fractionation is also absent in the highly fractionated residues [12] and this suggests fractionation via a refractory (or ultra-refractory) phase.

The high concentration of grossite in certain CAIs as well as the existence of silica-rich objects in CH chondrites point towards an effective removal of condensates from nebular gases during condensation, resulting in a fractionated residual nebular gas [14]. Although this could be a possible mechanism, the trouble with such fractional condensation scenarios is that different fractionation factors must be invoked to explain every individual object.

Because the main feature in the trace element patterns of the objects studied here is a variable depletions in HREE, coupled with variable depletions in Y, Sc and in the ultra-refractory Zr, the observed patterns could reflect condensation of the enstatite-rich liquids from a gas from which variable proportion of refractory phases had been removed. The positive Ce anomaly also suggests vapor fractionation.

In objects Acfer I, V and X the HREE abundances are more strongly depleted relative to the LREE, with all objects showing positive Yb, Nb, and Ce anomalies. These patterns suggest fractionation via a mineral phase enriched in HREE as well as Sc and Zr (hibonite, perovskite?) and are comparable to those found in Type II CAIs [e.g., 15] that - in addition - is very common among CAIs from CH chondrites [e.g., 16]. Removal of refractory elements (e.g., in Acfer I and V) seems to have occurred at very high temperatures as elements from Gd to Er show smoothly decreasing abundances, with Tm being the least abundant of all HREE. The positive Ce anomaly could be due to the redox-sensitive volatility of this element [e.g., 17-18]. One of the long-standing objections to the liquid condensation model is that it is hard to see how liquid condensation is compatible with the rapid cooling rates inferred from the textures of cryptocrystalline and radiating pyroxene chondrules. However, liquids can be formed metastably and therefore will crystallize instantaneously when a nucleus becomes available. The chondrules of this study seem to be a good example.

References: [1] Bischoff et al. (1993) *GCA 57*, 2631-2648. [2] Weisberg et al. (1988) *EPSL 91,* 19-31. [3] Scott (1988) *EPSL 9,* 1-18. [4] Wasson and Kallemeyn (1990) *EPSL 101*, 148-161. [5] Brearley and Layne (1995) *LPSC 26*, 167-168. [6] Russell et al. (2000) *MAPS 53* (Suppl.) A139. [7] Krot et al. (2000a) *LPSC 31*, #1481. [8] Krot et al. (2000b) *LPSC 31*, #1499. [9] Krot et al. (2002) *MAPS 37*, 1451-1490. [10] Krot et al. (2010) *GCA 74*, 2190-2211. [11] Hezel et al., (2003) *MAPS 38*, 1199-1215. [12] Floss et al.. (1996) *GCA 60*, 1975-1997. [13] Davis et al.. (1995) *LPSC 26*, 317-318. [14] Petaev and Krot (1999) *LPSC 30*, #1775. [15] Martin and Mason (1974), *Nature* 149, 333. [16] Weber and Bischoff (1994) *GCA 58,* 3855-3857. [17] Boynton, (1975) *GCA 39*, 569-584. [18] Davis et al. (1982) *GCA 46*, 1627-1651.